IEEE Access
Multidisciplinary | Rapid Review | Open Access Journal

Received January 7, 2021, accepted January 9, 2021, date of publication January 12, 2021, date of current version January 20, 2021.

*Digital Object Identifier 10.1109/ACCESS.2021.3051186*

# Research on Urban Load Rapid Recovery Strategy Based on Improved Weighted Power Flow Entropy

**MIN WANG[1], (Member, IEEE), ZONGYIN FAN[1], (Graduate Student Member, IEEE), JIAN ZHOU[2], AND SHANSHAN SHI[2]**

[1]College of Energy and Electrical Engineering, Hohai University, Nanjing 211100, China
[2]Electric Power Research Institute of State Grid Shanghai Electric Power Company, Shanghai 200437, China

Corresponding author: Zongyin Fan (642433783@qq.com)

This work was supported by the State Grid Shanghai Electric Power Company under Project B30940190004.

**ABSTRACT** As the final stage of power system restoration, the critical task of load restoration is to restore the remaining load as quickly as possible. With the continuous increase of the temperature-controlled load and the proportion of electric vehicle load in the urban power grid, the complexity of the load side in the restoration process gradually increases. Therefore, based on the existing grid environment, this paper considers the sudden increase in load recovery caused by cold load pick-up and the auxiliary effect of electric vehicle discharge on load recovery during the load recovery process. From the perspective of economy, safety, and speed, this paper establishes a multi-objective function that includes the amount of load, improved weighted power flow entropy, and the number of recovered lines. The multi-objective evolutionary algorithm based on decomposition is used to optimize the constructed multi-objective load recovery model. Through the IEEE30 node system, it is verified that the method proposed in this paper can effectively establish a fast and safe load recovery plan that meets the actual grid environment.

**INDEX TERMS** Load recovery, electric vehicle, cold load pick-up, improved weighted power flow entropy.

## I. INTRODUCTION

The power system restoration is divided into three stages: black start, grid reconstruction, and load recovery [1]. The primary purpose of load recovery as the final stage of power system restoration is to quickly and orderly recover the remaining load [2]. At present, domestic and foreign scholars' research on load recovery mainly focuses on four aspects: load recovery process modeling, load recovery strategy, objective function construction, and solution algorithm.

First of all, the modeling of the load recovery process mainly involves the classification and modeling of the load during the recovery process. In early studies, a fixed power is generally used to represent the load to be restored. However, as the penetration rate of temperature-controlled loads and electric vehicle loads in urban power grids is getting higher and higher, there are certain limitations in expressing the loads to be restored with a fixed power. During the load restoration stage, due to the loss of load diversity, the demand for electrical energy will suddenly rise. For this kind of situation, the overload phenomenon when the feeder switch is closed is called cold load pick-up (CLPU) [3]. The cold load pick-up will lead to slower load recovery and may even lead to secondary power outages. Therefore, in the study of load recovery, reference [4] proposed to divide the load types of the power system after a blackout into temperature-controlled load, human-controlled load, and fixed load, and established a linear probability model of the cold load pick-up characteristics of the temperature-controlled load; Reference [5] established a piecewise linear simplified model of cold load pick-up for the load recovery stage; Reference [6] adopted a cold load pick-up delay decay exponential model for the load recovery process. At the same time, with the increasing number of electric vehicles in cities and the development of V2G technology, reference [7], [8] considered the impact of electric vehicle discharge during the load recovery process, but did not consider the time characteristics of electric vehicle load connected to the grid.

Secondly, the current load recovery strategy mainly focuses on the sorting strategy of the load to be recovered.

The associate editor coordinating the review of this manuscript and approving it for publication was Zhigang Liu.

The priority of load recovery is usually set according to the importance of the load, so as to ensure the priority recovery of the important load, such as selecting the weight of load manually according to the load level or use the analytic hierarchy process to determine the comprehensive weight of the load [9], but both of these methods have a certain degree of subjectivity.

In addition, the goal of load recovery usually chooses the largest amount of load recovery as one of the objective functions [10], [11]. Reference [12] takes the user load interruption cost, resuming operation cost, and power generation cost as the goal. Reference [13] proposes the power flow entropy and takes it as one of the objective functions, which can quantitatively describe the imbalance of the power flow distribution of the line and analyze it as a representative system safety index. Reference [14] believes that the power flow entropy will be too large after the failure of some branches with heavy or light power flow. It is necessary to distinguish the weight of the power flow in the power flow entropy. Therefore, weighted power flow entropy is proposed to distinguish the line load rate. There is a shortcoming of insufficient sensitivity to heavy-load lines.

Finally, because the load recovery process is a multi-objective mathematical problem of mixed integer nonlinear programming, it is generally solved by the weighting method or swarm intelligence algorithm. Reference [15] uses the weighting method to convert the multi-objective function into a single objective function, but the weight setting of the weighting method has a certain subjective arbitrariness, and the weighting method still cannot solve the situation that the non-pareto front surface is a convex set and the distribution of the solution not evenly enough. The fast non-dominated sorting genetic algorithm with elite strategy (NSGA-II) adopted in [5] has a slower solution time, and at the same time, it is less effective in dealing with more than two objective functions, and it is easy to fall into a local optimum [16].

In summary, there are the following problems in the research of rapid load recovery after urban power grid failure: 1) The load to be recovered is represented by a fixed power, and there is a lack of consideration of the characteristics of the load during the recovery process; 2) The weight of the load point in the restoration process is relatively subjective and single; 3) Lack of consideration of the uneven distribution of line power flow, and when line power flow is unevenly distributed or part of the line load rate is too heavy, the system may enter a self-organized critical state, prone to secondary failures; 4) The solution method used needs to be improved.

In view of the above problems, this paper proposes the following solutions, which are the innovations of this paper: 1) Combining the characteristics of urban temperature- controlled and the increasing load of electric vehicles, this paper considers the sudden increase in load recovery caused by the cold load pick-up and the auxiliary recovery effect of electric vehicle discharge in the recovery process; 2) This paper proposes to combine the network cohesion and the amount of load, from the two aspects of network topology and the amount of load, to effectively evaluate the weight of the load point in the process of load recovery and the restoration priority of loads of different load levels are considered in the restoration process; 3) This paper proposes improved weighted power flow entropy and use it as one of the objective functions, which can optimize the distribution of network power flow during the load recovery process and strengthen the robustness of the load recovery process. At the same time, in the process of load recovery, this paper adjusts the objective function in stages according to the different recovery time steps so that the recovery strategy is more realistic; 4) In this paper, the multi-objective evolutionary algorithm based on decomposition (MOEA/D) is used to solve the multi-objective problem constructed in this paper. This algorithm has great advantages in maintaining the distribution of solutions and can effectively avoid fall into a local optimum.

It should be noted that a blackout accident is a small probability and a large damage event in the power grid. That is, the probability of occurrence is small, but it will cause a lot of losses. At present, the main research focuses on the simulation analysis and recovery plan design of a blackout accident in the power grid [17]–[20]. The research scenario in this paper is the load recovery after a blackout accident. Therefore, the method in this paper is mainly used to formulate a load recovery plan offline, which provides a certain reference for load recovery after a blackout accident.

## II. MODEL OF TYPICAL URBAN LOADS IN THE PROCESS OF LOAD RECOVERY

### A. COLD LOAD MODEL

#### 1) THE CONCEPT OF COLD LOAD PICK-UP

Usually, the temperature-controlled load will stop running after reaching the set temperature. At this time, although the temperature-controlled load ratio is relatively high, not all temperature-controlled loads are in operation, and the system has a high load diversity. Load diversity usually refers to the power value obtained by subtracting the peak loads of the above loads from the sum of the peak loads of two or more loads in a period of time. It is mainly used to characterize the difference of operating status of load [21].

After a blackout accident, the temperature-controlled load will be started synchronously. At this time, the loss of load diversity will cause the load to be restored at the initial stage of recovery to be much larger than the steady-state load. This phenomenon is called cold load pick-up. After that, as the load gradually recovers, its load diversity is gradually restored, and the load will gradually attenuate to the normal load according to a certain attenuation rate.

#### 2) DELAY DECAY EXPONENT MODEL

Because of the long-term nature of the load recovery process and the feasibility of analysis and calculation, this paper uses the delayed decay exponential model of [6] to study the cold load pick-up.

According to Figure 1, the change law of load during the cold load pick-up process can be expressed as follow:

$$P(t) = [P_0 + (P_{peak} - P_0)e^{-\alpha(t-t_1)}]u(t - t_1) \quad (1)$$

where $P(t)$ is the power function during the process of cold load pick-up; $P_0$ is the load power at the normal time; $P_{peak}$ is the peak power of the load; $t_1$ is the beginning time of attenuation; $t_2$ is the moment when the load decrements to the normal load; $\alpha$ is cold load attenuation factor; $u(t)$ is the unit step function.

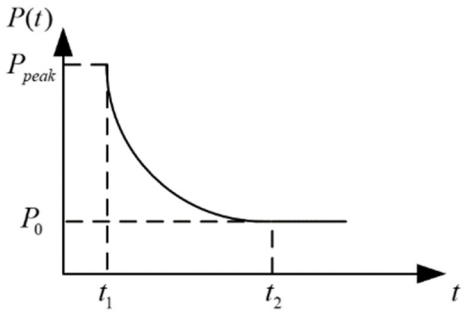


**FIGURE 1.** Model of cold load pick-up.

### B. ELECTRIC VEHICLE CHARGING AND DISCHARGING POWER MODELING

#### 1) PROBABILITY MODELING OF ELECTRIC VEHICLE RETURN TIME AND DAILY MILEAGE

Existing research shows that most private electric vehicles are idle for most of the day. Therefore, as a mobile distributed energy storage resource [22], electric vehicles can participate in the recovery of power systems after a power system blackout occurs [23], [24].

In order to obtain the charge and discharge power of an electric vehicle at any time, it is first necessary to model the probability characteristics of the return time and the daily mileage of the electric vehicle.

According to [25], the return time of electric vehicles meets the normal distribution, with expectation $\mu_s = 17.6$; standard deviation $\sigma_s = 3.4$, and the probability density function is as follows:

$$f_s = \begin{cases} \frac{1}{\sigma_s\sqrt{2\pi}} \exp[\frac{(x-\mu_s)^2}{2\sigma_s^2}], & (\mu_s - 12) < x \le 24 \\ \frac{1}{\sigma_s\sqrt{2\pi}} \exp[\frac{(x+24-\mu_s)^2}{2\sigma_s^2}], & 0 < x \le (\mu_s - 12) \end{cases} \quad (2)$$

where $x$ is the return time of the electric vehicle.

The daily mileage of electric vehicles meets the lognormal distribution, with expectation $\mu_D = 3.2$; standard deviation $\sigma_D = 0.88$, and the probability density function is as follows:

$$f_D = \frac{1}{y\sigma_D\sqrt{2\pi}} \exp[-\frac{(\ln y - \mu_D)^2}{2\sigma_D^2}] \quad (3)$$

where $y$ is the daily mileage of electric vehicle.

#### 2) ELECTRIC VEHICLE CHARGE AND DISCHARGE POWER

Theoretically, the charging and discharging power of electric vehicles can be expressed as follow:

$$P_{EV,CH}(t) = \sum_{i=1}^{N_{EV}(t)} P_{ev,ch}(i, t) \quad (4)$$

$$P_{EV,DIS}(t) = \sum_{i=1}^{N_{EV}(t)} P_{ev,dis}(i, t) \quad (5)$$

where $N_{EV}(t)$ is the number of electric vehicles charging and discharging in the electric vehicle charging station at the time $t$; $P_{ev,ch}(i, t)$ and $P_{ev,dis}(i, t)$ are respectively the maximum charging and discharging power of electric vehicle $i$ at the time $t$.

In practice, when charging and discharging electric vehicles, the maximum charging and discharging power cannot always be maintained. The charging and discharging power of an electric vehicle are related to the state-of-charge (SOC) of the battery when charging or discharging. Therefore, (4) and (5) need to be corrected as follow [26]:

$$P_{EV,CH}(t) = \beta_{ch}(t) \sum_{i=1}^{N_{EV}(t)} P_{ev,ch}(i, t) \quad (6)$$

$$P_{EV,DIS}(t) = \beta_{dis}(t) \sum_{i=1}^{N_{EV}(t)} P_{ev,dis}(i, t) \quad (7)$$

$$\beta_{ch}(t) = 1 - \sqrt{\frac{E_{EV}(t)}{N_{EV}(t) \cdot Q_N}} \quad (8)$$

$$\beta_{dis}(t) = \sqrt{\frac{E_{EV}(t)}{N_{EV}(t) \cdot Q_N}} \quad (9)$$

where $\beta_{ch}(t)$ and $\beta_{dis}(t)$ are the adjustment coefficients of battery charging and discharging power of EVs at the time $t$; $E_{EV}(t)$ is the remaining battery of electric vehicles in charging and changing station at the time $t$; $Q_N$ is the rated capacity of EVs battery; the result of dividing $E_{EV}(t)$ by $N_{EV}(t) \cdot Q_N$ in equation (8) and (9) is the SOC of electric vehicles, so the essence of the adjustment coefficient is to use the SOC of electric vehicles to roughly estimate the proportion of the number of electric vehicles that can participate in charging and discharging to the total number of electric vehicles.

## III. LOAD RECOVERY STRATEGY

The essence of load recovery is the nonlinear integer optimization problem of 0-1 combination. In this stage, the residual load should be recovered as much as possible on the basis of the backbone network frame established in the network frame reconstruction stage. Its objective function can be expressed as follows:

$$f_1 = \sum_{i=1}^{N} c_i \lambda_i L_i \quad (10)$$

where $N$ is the number of system nodes; $c_i$ is the node switch case, 0 means the node switch is off, 1 means the node switch

is closed; $\lambda_i$ is the node importance coefficient; $L_i$ is the load of the node to be recovered.

Reference [27] uses network cohesion to evaluate the importance of nodes in the process of skeleton network reconstruction, which can objectively reflect the importance of nodes in the network. Therefore, this paper uses the product of the network cohesion after node contraction and the load to be restored to express the node importance coefficient, which is defined as follows:

$$\begin{cases} \lambda_i = \alpha_i L_i \\ \alpha_i = 1/n_i l_i \\ l_i = \sum\limits_{a,b \in V} d_{\min,ij}/[n_i(n_i-1)/2] \end{cases} \tag{11}$$

where $\alpha_i$ is the network aggregation degree; $L_i$ is the load of the node to be recovered; $n_i$ is the number of nodes in the network after node $i$ contraction; $l_i$ is the average shortest path between nodes after node $i$ contraction; $d_{\min,ij}$ is the shortest distance between any two nodes in the contracted network expressed by the number of edges; $V$ is a collection of all the nodes in a network.

Considering that the load of some nodes to be restored is small, but its importance is high, this paper divides the load of nodes to be restored into first-level, second-level, and third-level loads and sets corresponding weights as 100, 10, and 1, respectively. The specific weight setting can be adjusted according to actual needs. The improvement of (10) is as follows:

$$f_1' = \sum_{i=1}^{N} c_i w_i (100 L_{i1} + 10 L_{i2} + L_{i3}) \tag{12}$$

## IV. OTHER OBJECTIVE FUNCTIONS

### A. IMPROVED WEIGHTED POWER FLOW ENTROPY

In the process of load recovery, some lines will have a high load rate, that is, overload. The reasons for this phenomenon mainly include two aspects: on the one hand, the node in normal operation often has multiple lines to supply power to the load on the node. In the process of load recovery, the line connected to the load point cannot be recovered at the same time. Therefore, the load on the recovered line will be overloaded; on the other hand, if there is more temperature-controlled load on the node to be recovered, then due to the influence of cold load pick-up, the load of the node to be restored will increase suddenly, and the line load rate will also be too high.

Entropy is one of the parameters that characterize the state of matter in thermodynamics, and its physical meaning is a measure of the degree of chaos in the system. The power flow entropy of the power system is mainly used to quantitatively evaluate the uniformity of the line load distribution. The smaller the power flow entropy, the more uniform the line load distribution, and vice versa [28].

It can be seen that in the process of load recovery, the increase in line load rate caused by load input is a major safety hazard during the recovery process. Although the traditional line average load factor can reflect the overall load level as a whole, it does not consider the impact of uneven distribution of line power flow. Therefore, the power flow entropy is introduced to quantitatively describe the distribution of the line power flow during the load restoration process and to evaluate the safety of the restoration process.

Assuming that the maximum load capacity of the line $l_i$ is $F_i^{\max}$, and the line power flow in actual operation is $F_i^0$, the load factor $\eta$ of the line is:

$$\eta = \left| \frac{F_i^0}{F_i^{\max}} \right| \tag{13}$$

According to the line load rate limit, divide the line load rate interval into continuous equal difference intervals $D = [D_0, D_1, \ldots, D_n]$, $D_n$ can be set according to the actual operation requirements of the network [29]. The probability that the load rate of the line $i$ is in the interval $(D_k, D_{k+1}]$ is $P(X_i)$, power flow entropy is defined as follows:

$$H(k) = -C \sum_{i=1}^{M} P(X_i) \ln P(X_i) \tag{14}$$

where $C$ is a constant; $M$ is the total number of lines.

When the traditional power flow entropy is small, it is impossible to distinguish whether it is caused by high or low line load rate. Although the latter will not have an adverse effect on the grid, for the former, too high line load rate may lead to secondary failures in the recovery process or the interruption of the recovery process.

Reference [14] uses weighted power flow entropy to effectively distinguish the degree of line load, which is defined as follows:

$$H(k) = -\sum_{i=1}^{M} w_i P(X_i) \ln P(X_i) \tag{15}$$

$$w_i = \frac{P_i - P_{\min}}{P_{\max} - P_{\min}} \tag{16}$$

where $w_i$ is the weight coefficient used to distinguish the line load; $P_i$ is the actual active power flow value of the line $i$; $P_{\max}$ and $P_{\min}$ are the maximum and minimum active power flow values of the line $i$, respectively.

According to (16), it can be found that the weight coefficient of power flow entropy is always less than 1. Although the influence of line load degree is divided, it is still not sensitive enough to reflect the heavy load line, especially the line that exceeds the limit is not distinguished enough.

Therefore, this paper proposes an improved weighted power flow entropy, and its weight coefficient is calculated as follows:

$$w_i' = \left(\frac{P_i - P_{\min}}{\kappa P_N - P_{\min}}\right)^2 \tag{17}$$

where $P_i$ is the actual active power flow value of the line $i$; $P_{\min}$ is the minimum active power flow value of the line $i$; $\kappa$ is the line load rate limit coefficient, which is mainly related

to the wiring method of the line; $P_N$ is the limit transmission power of the line, which is mainly determined by the thermal stability of the wire.

It can be seen from (17) that if the line load exceeds the limit, the value of $w_i'$ will be greater than 1, and then the squaring process will make the power flow entropy weight of the line larger, thereby better limiting the appearance of the line with the load limit.

Therefore, combined with (15), the calculation formula of the improved weighted power flow entropy can be obtained as follows:

$$f_2 = H(k) = -\sum_{i=1}^{M} w_i' P(X_i) \ln P(X_i) \tag{18}$$

### B. NUMBER OF RESTORED LINES

Taking the minimum number of lines to be restored during the load restoration process as the objective function can reduce the complexity and risk of system restoration operations and ensure the rapidity of the load restoration process. For a system with $M$ lines, the objective function can be defined as follows:

$$f_3 = A^T A \tag{19}$$

where $A = [a(1), a(2), \ldots, a(M)]^T$ is the binary decision vector of $M \times 1$ dimension, represents the network connection in the load recovery process, and $a(i) \in \{0, 1\}$, $i = 1, 2, \ldots, M$.

In the process of load restoration, there is a certain contradiction between restoring as much load as possible to ensure the economy and restoring as few lines as possible to ensure rapidity. Therefore, in the first-time step of load recovery, this paper requires that important loads be restored first and the speed is as fast as possible, while in the other time steps, it is required to restore as much load as possible and also hope to restore as many lines as possible, which makes the load recovery strategy more reasonable, shown as follow:

$$f_3' = \begin{cases} A^T A & k = 1 \\ -A^T A & k \neq 1 \end{cases} \tag{20}$$

where $k$ is the time step of load recovery, when $k = 1$ means the current time step is the first time step of load recovery.

## V. LOAD RECOVERY PROCESS MODEL

### A. MULTI-OBJECTIVE FUNCTION MODEL

According to Section III and Section IV, the multi-objective function established in this paper is as follows:

$$f = \left\{\max f_1', \min f_2, \min f_3'\right\} \tag{21}$$

where $f$ is the objective function to be optimized; $f_1'$, $f_2$ and $f_3'$ respectively correspond to the weighted load recovery, the improved weighted power flow entropy, and the number of restored lines.

### B. CONSTRAINT CONDITIONS

#### 1) LINE POWER FLOW CONSTRAINT

Load recovery needs to consider line power flow constraint:

$$\begin{cases} \Delta P_i = P_i - U_i \sum_{j=1}^{N} U_j (G_{ij} \cos\theta_{ij} + B_{ij} \sin\theta_{ij}) = 0 \\ \Delta Q_i = Q_i - U_i \sum_{j=1}^{N} U_j (G_{ij} \sin\theta_{ij} - B_{ij} \cos\theta_{ij}) = 0 \end{cases} \tag{22}$$

where $P_i$ and $Q_i$ are the active and reactive injection power of node $i$ respectively; $U_i$ is the voltage of node $i$; $G_{ij}$ and $B_{ij}$ are the conductance and susceptance between node $i$ and node $j$, respectively.

#### 2) GENERATOR OUTPUT CONSTRAINT

In the process of load recovery, the recoverable load at the current time step is related to the sum of the power provided by the generator at the time step. The recovered load should meet the generator output constraint, shown as follow:

$$\Delta P_L \leq \Delta P_G \tag{23}$$

where $\Delta P_L$ is the load recovered at the current time step; $\Delta P_G$ is the increase of current time-stepping generator output, shown as follow:

$$\Delta P_G = \sum_{j=1}^{s} [P_{Gj}(t + \Delta t) - P_{Gj}(t)] \tag{24}$$

where $s$ is the number of generators in the system; $\Delta t$ is the step length; $P_{Gj}(t)$ is the active power of the unit $j (j = 1, \ldots, s)$ at the moment $t$, which can be determined by the simplified starting curve of the unit as shown in Figure 2.

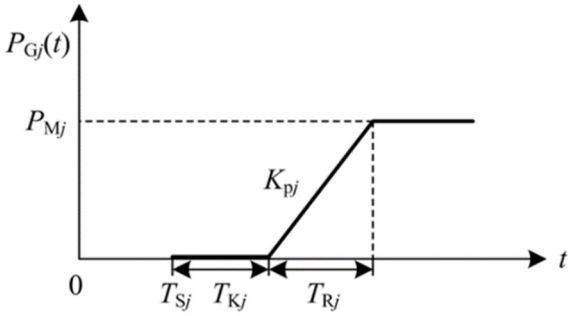


**FIGURE 2.** Chart of generation output.

As shown in Figure 2, $P_{Gj}(t)$ can be calculated as follow:

$$P_{Gj}(t) = \begin{cases} 0 & 0 \leq t \leq T_{Sj} + T_{Kj} \\ K_{Pj}(t - T_{Sj} - T_{Kj}) & T_{Sj} + T_{Kj} < t \leq T_{Sj} + T_{Kj} + T_{Rj} \\ P_{Mj} & T_{Sj} + T_{Kj} + T_{Rj} < t \end{cases} \tag{25}$$

where $T_{Sj}$ is the starting time of the unit $j$; $T_{Kj}$ is the time required for the output power of the unit $j$ from start to start climbing; $T_{Rj}$ is the time required for the unit $j$ to climb from the beginning to the maximum output power; $K_{Pj}$ is the climbing slope of the unit $j$; $P_{Mj}$ is the rated power of the unit $j$.

#### 3) SINGLE INPUT MAXIMUM LOAD CONSTRAINT

In the load recovery process after the power system blackout, the constant input load is equivalent to the system disturbance and then the readjustment process. To ensure the stability of the system in the whole load recovery process, the constraint of the maximum load of a single input is considered to prevent the risk of new system instability caused by the excessive load of a single input.

According to the rated power and frequency response value of the grid-connected generator of the system, the maximum load that can be input in the current time step can be roughly calculated:

$$\Delta P_L \leq \Delta P_{L\max} \tag{26}$$

$$\Delta P_{L\max} = \Delta f_{\max} \sum_{j=1}^{s} \frac{P_{Nj}}{df_j} \tag{27}$$

where $\Delta P_L$ is the load restored at the current time step; $\Delta P_{L\max}$ is the maximum load that can be put into operation at the current time step, and its value can be calculated according to the rated power and frequency response of the grid-connected generators $\Delta f_{\max}$ is the maximum allowable value of system frequency reduction; $P_{Nj}$ is the rated active power of the unit $j$; $df_j$ is the frequency response value of the unit $j$ under the current load rate.

#### 4) OTHER INEQUALITY CONSTRAINTS

$$P_{Gi\min} \leq P_{Gi} \leq P_{Gi\max} \quad i = 1, 2, \ldots N_G \tag{28}$$

$$Q_{Gi\min} \leq Q_{Gi} \leq Q_{Gi\max} \quad i = 1, 2, \ldots N_G \tag{29}$$

$$U_{i\min} \leq U_i \leq U_{i\max} \quad i = 1, 2, \ldots, N \tag{30}$$

where $P_{Gi}$ and $Q_{Gi}$ are the active power and reactive power of the generator, respectively; $N_G$ is the number of generators; $U_i$ is the node voltage.

## VI. SOLUTION OF MODEL

In the process of load recovery, 0/1 is usually used to represent the disconnection and recovery of the line, so its essence is a mixed integer programming problem with multiple objectives and multiple constraints. This paper uses the MOEA/D algorithm to solve. This method was proposed by Qingfu Zhang in 2007 [30]. Compared with other multi-objective algorithms, MOEA/D has the following characteristics:

(1) MOEA/D algorithm optimates the N-scalar problem simultaneously rather than solving the multi-objective optimization problem as a whole, so MOEA/D will reduce the difficulty of diversity maintenance and fitness allocation of traditional MOEA.

(2) MOEA/D uses the solution information of adjacent subproblems to simultaneously optimize N-scalar problems. Relatively speaking, MOEA/D does not repeat optimization for scalar subproblems because it utilizes the coevolution mechanism between subproblems, so the computational complexity of the algorithm is relatively low.

Generally, the commonly used methods for converting a multi-objective problem into a set of scalar optimization problems include: the weighted sum approach, the Chebyshev approach, and the penalty-based boundary intersection approach. The MOEA/D algorithm uses the Chebyshev approach. The following only introduces the Chebyshev approach:

The Chebyshev approach transforms the problem into the following scalar problem:

$$\begin{aligned} &\min g^{ch}(x|\lambda, z^*) = \max\{\lambda_i(f_i(x) - z_i^*)\} \\ &s.t.\ x \in \Omega \end{aligned} \tag{31}$$

where $z^* = (z_1^*, z_2^*, \ldots, z_m^*)^T$, for each target component $i$, $z_i^* = \min\{f_i(x)|x \in \Omega\}$ that is, the ideal solution consisting of the minimum value of each target component.

The main steps of the load recovery process using the MOEA/D algorithm are as follows:

### A. SETTING PARAMETERS

Set the number of objective functions $m$; set the population size $N$; generate uniformly distributed weight vectors $\{\lambda^1, \lambda^2, \ldots, \lambda^N\}$, the number of weight vectors is $N$; set the number of weight vectors in each neighborhood $T$; set the number of algorithm iterations.

### B. INITIALIZATION

Step2.1: Calculate the Euclidean distance between any two weight vectors, find the $T$ weight vectors closest to each weight vector. For each $i = 1, 2, \ldots, N$, let $B(i) = \{i_1, i_2, \ldots, i_T\}$, $\lambda^{i_1}, \lambda^{i_2}, \ldots, \lambda^{i_T}$ are the $T$ weight vectors closest to $\lambda^i$;

Step2.2: The code is coded according to the recovery of the system network frame. 0 means the line is disconnected, 1 means the line is connected, and the dimension of chromosome is the number of bus routes. Initial chromosome population is randomly generated $\{x^1, x^2, \ldots, x^N\}$, and one chromosome $x$ corresponds to a load recovery scheme;

Step2.3: Perform power flow calculation on the generated initial population. If the power flow calculation converges, the fitness value of the individual is obtained; otherwise, the fitness value of the individual is set to a larger real number $p$;

Step2.4: Initialize the ideal solution set $z = \{z_1, z_2, \ldots z_m\}$, let $z_i = \min\{f_i(x^1), f_i(x^2), \ldots, f_i(x^2)\}$;

Step2.5: Initialization set $EP$, used to store all non-dominated solutions, initially empty.

### C. UPDATE

Step3.1: Circulate according to the set number of iterations, randomly select two serial numbers $k$ and $l$ from $B(i)$, cross-mutate the corresponding individuals $x^k$ and $x^l$ to generate a new solution $y$, and calculate a new fitness value;

Step3.2: Update the ideal solution $z$. For all $j = 1, 2, \ldots, m$, if $z_j < f_j(y)$ then set $z_j = f_j(y)$;

Step3.3: Update the neighborhood solution. For $j \in B(i)$, if $g^{ch}(y|\lambda^j, z) \leq g^{ch}(x^j|\lambda^j, z)$, then set $x^j = y$;

Step3.4: Update $EP$. Remove all solutions dominated by $f(y)$ from $EP$. If all solutions in $EP$ do not dominate $f(y)$, add $f(y)$ to $EP$;

Step3.5: Complete a cycle and the number of iterations increases by one.

### D. STOP CRITERION

Whether the number of iterations is reached, stop and output if yes, otherwise go to step3 to update.

The algorithm flow chart is shown in Figure 3.

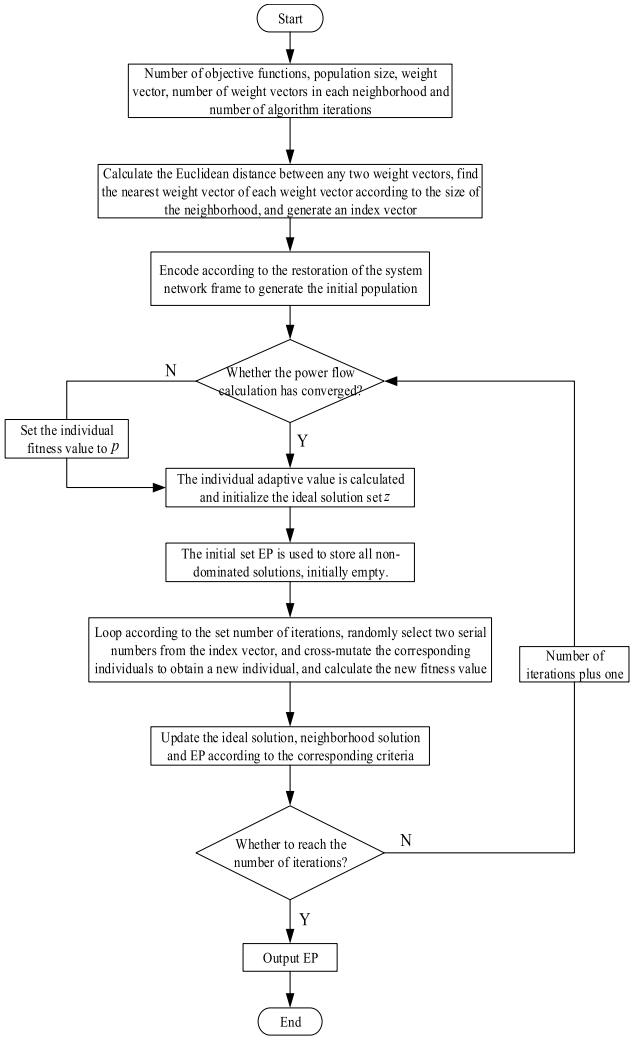


**FIGURE 3.** Flow chart of the algorithm.

## VII. ANALYSIS OF EXAMPLE

The computer used in this article is Lenovo-S41, Intel(R) Core(TM) i5-5200U CPU@ 2.20GHz and the programming software used in this article is Matlab2018a. This paper uses the IEEE30-node system shown in Figure 4 as an example after completing the network frame reconstruction to verify the method in this paper. The isolated node is the node to be restored. The frequency response parameters and node parameters of the generator are shown in Table 1 and Table 2. In order to simplify the calculation, the other parameters are set as follows: this paper takes the climbing power of the generator set composed of all power generation as 87MW/h; it is generally believed that the input load should not reduce the system frequency by more than 0.5Hz. In order to ensure the stability of the frequency, the maximum frequency reduction is 0.3Hz; LJG-300 is selected as the wire model, its thermal stability limit transmission current is 700A, $\kappa$ takes 0.9; the number of electric vehicles is 1000, according to the probability model of electric vehicles established in section 2.2, using Monte Carlo method to extract the initial charging time and daily mileage of each sample, and calculate the number of electric vehicles charged and discharged. This article selects the Nissan SYLPHY electric vehicle model. The battery is a sheet-type high-performance ternary lithium-ion battery with a battery capacity of 38kWh, a charging power of 6.60kW, and a discharge power of 5.86kW.

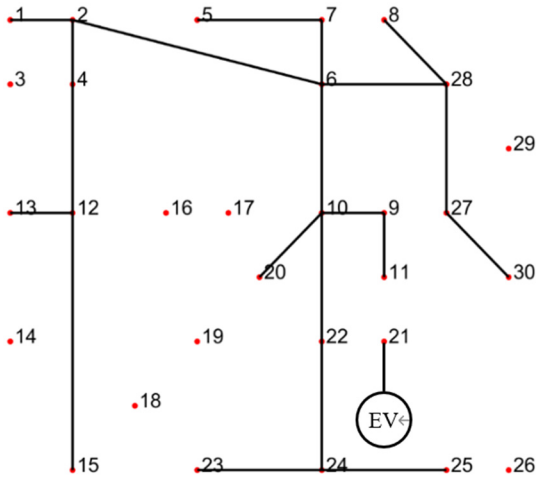


**FIGURE 4.** The system diagram after the reconfiguration of the grid.

**TABLE 1.** Parameters of the units.

| Node number | $P_G$ /MW | Frequency response values at different load rates /（Hz/p.u.） | | |
|---|---|---|---|---|
| | | 5% | 40% | 75% |
| 1 | 200 | -5.35 | -3.4 | -1.46 |
| 2 | 80 | -4.81 | -4.61 | -4.41 |
| 5 | 50 | -8.56 | -7.94 | -7.33 |
| 8 | 60 | -8.56 | -7.94 | -7.33 |
| 11 | 30 | -8.56 | -7.94 | -7.33 |
| 13 | 40 | -8.56 | -7.94 | -7.33 |

Table 1 shows the frequency response values of a typical generator set under load rates of 5%, 40%, and 75%. Piecewise linear interpolation method is used to calculate the frequency response values of a generator set under different load rates.

Table 2 shows the parameters of the nodes to be restored. Taking into account the characteristics of urban loads, this paper divides the nodes to be restored into three categories: industrial, commercial, and civil. Among them,

**TABLE 2.** Parameters of nodes to be restored.

| Node number | Load/MW | Load level | Load ratio/% | Cold load ratio/% |
|---|---|---|---|---|
| 3(civil) | 2.4 | Level 1 | 0 | 40 |
| | | Level 2 | 20 | |
| | | Level 3 | 80 | |
| 14(industry) | 6.2 | Level 1 | 70 | 10 |
| | | Level 2 | 20 | |
| | | Level 3 | 10 | |
| 16(civil) | 3.5 | Level 1 | 10 | 40 |
| | | Level 2 | 30 | |
| | | Level 3 | 60 | |
| 17(industry) | 9 | Level 1 | 80 | 10 |
| | | Level 2 | 10 | |
| | | Level 3 | 10 | |
| 18(civil) | 3.2 | Level 1 | 0 | 40 |
| | | Level 2 | 20 | |
| | | Level 3 | 80 | |
| 19(commerce) | 9.5 | Level 1 | 0 | 30 |
| | | Level 2 | 50 | |
| | | Level 3 | 50 | |
| 21(civil) | 17.5 | Level 1 | 0 | 30 |
| | | Level 2 | 20 | |
| | | Level 3 | 80 | |
| 26(commerce) | 3.5 | Level 1 | 10 | 20 |
| | | Level 2 | 60 | |
| | | Level 3 | 30 | |
| 29(commerce) | 2.4 | Level 1 | 10 | 20 |
| | | Level 2 | 50 | |
| | | Level 3 | 40 | |

the industrial load contains more primary loads and needs to be restored first. Commercial loads contain more secondary loads; civil loads contain more tertiary loads, of which cold load accounts for a higher proportion of civil and commercial loads but lower in industrial loads. This setting is also in line with the relatively high proportion of temperature control loads in civil and commercial loads, such as air conditions.

### *A. EXAMPLE ANALYSIS AND DISCUSSION*

Taking into account the complexity and variability of the load recovery site, it takes about 5-15 minutes for a node to recover from an isolated state to full load recovery. The time step is taken in the calculation process, and the specific time step can be set according to the actual needs of the site.

#### 1) COMPARISON OF ALGORITHM

Using MOEA/D for load recovery calculation, the population size of the algorithm is 50, the evolutionary algebra is 50, the crossover probability is 0.9, and the mutation probability is 0.024. Therefore, this paper selects the non-dominated sorting Genetic Algorithms (NSGA-II) to compare with the algorithm used in this paper. The optimal results obtained by NSGA-II and the results of the MOEA/D algorithm are shown in Table 3.

According to the analysis in Table 3, the calculation time of the algorithm in this paper is significantly shortened, and a more reasonable load recovery plan can be obtained. That is, important loads can be recovered faster.

**TABLE 3.** Comparison of the algorithm.

| Timestep | Load level | NSGA-II | The algorithm of this paper |
|---|---|---|---|
| First-time step | Primary load/MW | 9.5081 | 13.4615 |
| | Secondary load/MW | 8.6334 | 4.7237 |
| | Third load/MW | 13.8601 | 5.9556 |
| Second-time step | Primary load/MW | 4.9471 | 0.5458 |
| | Secondary load/MW | 8.1569 | 9.3791 |
| | Third load/MW | 7.4502 | 14.0110 |
| Third-time step | Primary load/MW | 0 | 0.4479 |
| | Secondary load/MW | 4.1761 | 6.8637 |
| | Third load/MW | 16.7046 | 18.0484 |
| Calculating time/s | | 469.9 | 226.3 |

**TABLE 4.** Comparison of recovery strategies.

| Recovery strategy | Objective function |
|---|---|
| 1 | $f_1$、$f_2$、$f_3$ |
| 2 | $f_1'$、$f_2$、$f_3$ |
| 3 | $f_1$、$f_2$、$f_3'$ |
| 4 | $f_1'$、$f_2$、$f_3'$ |

#### 2) VERIFICATION OF RECOVERY STRATEGY

In order to verify the effectiveness of the recovery strategy proposed in this article, different recovery strategies are formed by setting different objective functions, and the results are compared, as shown in Table 4 and Figure 5, 6, 7, and 8.

By comparing the load recovery plan in Figure 5 and Figure 6, it can be found that considering the load level during the load recovery process, the primary load can be restored in the first time. If the traditional load recovery objective function is adopted, the primary load recovery process will be delayed.

Comparing Figure. 5 and Figure. 7, it can be found that compared with recovery strategy 1, recovery strategy 3 only needs three time steps to complete the restoration. Therefore, only consider the restoration of as few lines as possible during the first time step of load restoration. Restoring as many lines as possible at other times can speed up the process of load restoration.

Figure 8 is the recovery strategy adopted in this article. Compared with other strategies, while ensuring the rapid recovery, most of the important loads can also be recovered in

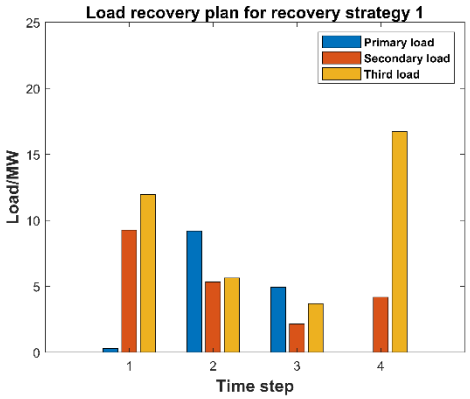


**FIGURE 5.** Load recovery plan of recovery strategy 1.

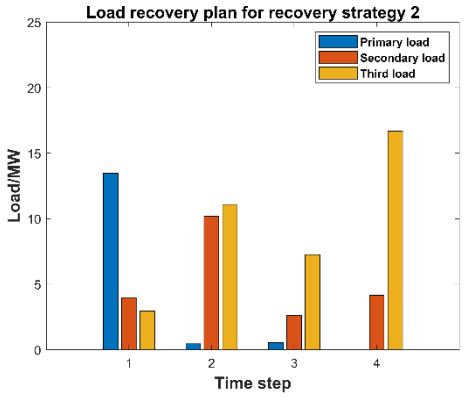


**FIGURE 6.** Load recovery plan of recovery strategy 2.

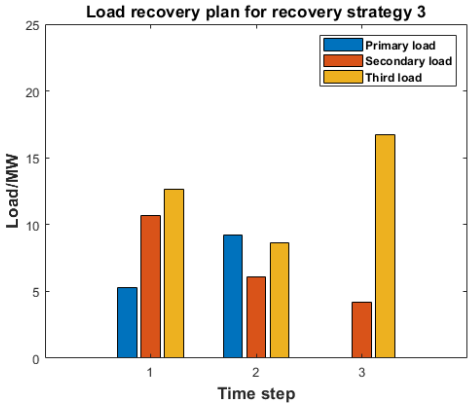


**FIGURE 7.** Load recovery plan of recovery strategy 3.

the first time, taking into account the requirements of rapidity and economy.

### 3) VERIFICATION OF IMPROVED WEIGHTED POWER FLOW ENTROPY

In order to verify the limiting effect of the improved weighted power flow entropy on the line over-limit power flow in load recovery, the line load rate at the end of the first time step is used for comparison. The result is shown in Figure 9. It can be seen that the weighted power flow entropy and the improved weighted power flow entropy has obvious limitation on the line overload during the restoration process.

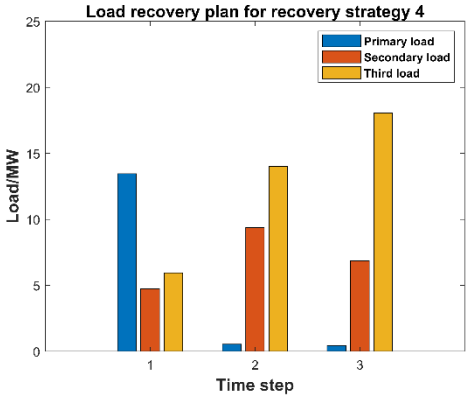


**FIGURE 8.** Load recovery plan of recovery strategy 4.

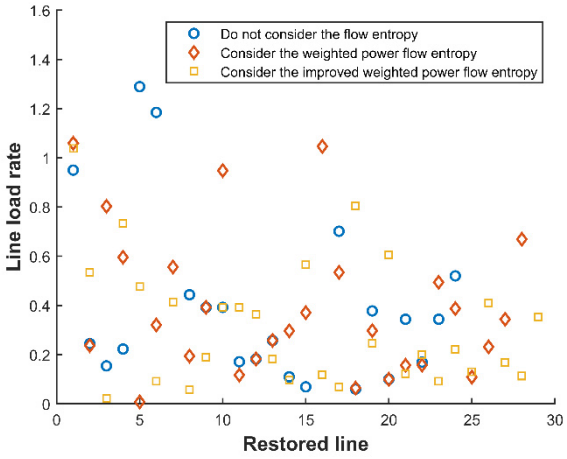


**FIGURE 9.** Load recovery plan of recovery strategy 4.

Analyzing the results at the end of the first time step, we can get that without considering the improvement of power flow entropy, the distribution variance of the line load rate is 0.438, of which there are 3 lines with the line load rate exceeding 90%; When considering the weighted power flow entropy, the distribution variance of the line load rate is 0.287, of which there are 3 lines with the line load rate exceeding 90%; When considering the improved weighted power flow entropy, the distribution variance of the line load rate is 0.248, of which there is one line with the line load rate exceeding 90%. Through the above analysis, it can be seen that when the improved weighted power flow entropy proposed in this paper is considered, the uniformity of the line power flow distribution has been further improved, and the number of lines with over-load is less.

## VIII. CONCLUSION

This paper starts from the backbone grid that has completed the grid reconfiguration after the blackout. First, the typical urban load is analyzed during the load recovery process, taking into account the influence of the cold load pick-up characteristics and the auxiliary role of electric vehicle discharge; second, evaluate the importance of load nodes to be restored based on the degree of network cohesion and

the amount of load, and consider the restoration priorities of loads of different load levels during the restoration process; third, an improved weighted power flow entropy is proposed, which can better distinguish between light-load and heavy-load lines in the system, so as to prevent the appearance of heavy-load lines from affecting load recovery. At the same time, considering that the objective function changes with the recovery time step, a more reasonable and effective load recovery strategy is proposed; Finally, the multi-objective evolutionary algorithm based on decomposition is used to solve the constructed multi-objective and multi-constrained load recovery problem. Compared with other algorithms, the superiority of this algorithm is demonstrated. The IEEE30-node system example is used to verify the effectiveness of the method proposed in this paper.

## REFERENCES


[1] M. M. Adibi and R. J. Kafka, "Power system restoration issues," *IEEE Comput. Appl. Power*, vol. 4, no. 2, pp. 19–24, Apr. 1991.

[2] M. M. Adibi and L. H. Fink, "Power system restoration planning," *IEEE Trans. Power Syst.*, vol. 9, no. 1, pp. 22–28, Feb. 1994.

[3] D. R. Medina, E. Rappold, O. Sanchez, X. Luo, S. R. R. Rodriguez, D. Wu, and J. N. Jiang, "Fast assessment of frequency response of cold load pickup in power system restoration," *IEEE Trans. Power Syst.*, vol. 31, no. 4, pp. 3249–3256, Jul. 2016.

[4] H.-B. Qu, "Studies on load restoration after power system major blackout," Ph.D. dissertation, Shandong Univ., Jinan, China, Apr. 2012.

[5] X.-P. Gu, B.-B. Zhao, and W.-X. Liu, "Load restoration based on multi-objective optimization and grey incidence decision-making," *Electr. Power Automat. Equip.*, vol. 35, no. 9, pp. 6–13, Sep. 2015.

[6] K. P. Schneider, E. Sortomme, S. S. Venkata, M. T. Miller, and L. Ponder, "Evaluating the magnitude and duration of cold load pick-up on residential distribution using multi-state load models," *IEEE Trans. Power Syst.*, vol. 31, no. 5, pp. 3765–3774, Sep. 2016.

[7] L. Sun, Z. Lin, M. A. Salam, X. Wang, F. Wen, S. P. Ang, and W. Liu, "Optimisation model for power system restoration with support from electric vehicles employing battery swapping," *IET Gener., Transmiss. Distrib.*, vol. 10, no. 3, pp. 771–779, Feb. 2016.

[8] Y. Wang, M. Yao, L. Chen, and X. Li, "Islanding strategy for restoring electric power supply by means of electric vehicle idle power against cold load pickup," *IET Gener., Transmiss. Distrib.*, vol. 13, no. 5, pp. 613–625, Mar. 2019.

[9] X. Gu and H. Zhong, "Optimisation of network reconfiguration based on a two-layer unit-restarting framework for power system restoration," *IET Gener., Transmiss. Distrib.*, vol. 6, no. 7, pp. 693–700, Jul. 2012.

[10] M. Ott, M. AlMuhaini, and M. Khalid, "A MILP-based restoration technique for multi-microgrid distribution systems," *IEEE Access*, vol. 7, pp. 136801–136811, 2019.

[11] L.-J. Yang, Y. Zhao, C. Wang, P. Gao, and J.-H. Hao, "Resilience-oriented hierarchical service restoration in distribution system considering microgrids," *IEEE Access*, vol. 7, pp. 152729–152743, 2019.

[12] A. Arab, A. Khodaei, S. K. Khator, and Z. Han, "Electric power grid restoration considering disaster economics," *IEEE Access*, vol. 4, pp. 639–649, 2016.

[13] W.-X. Liu, X.-P. Gu, J.-Y. Wang, and B.-B. Zhao, "Optimization of load recovery scheme considering system security factors," *Automat. Electr. Power Syst.*, vol. 40, no. 12, pp. 93–97, Jun. 2016.

[14] M.-C. Li, W.-M. Mei, Y.-Q. Liu, L.-K. Zhang, D.-W. Song, and C. Zhao, "Accurate identification method of brittle branches in power grid based on improved load flow entropy indexes," *Power Syst. Technol.*, vol. 43, no. 3, pp. 1026–1033, Mar. 2019.

[15] W. Gong, J.-Y. Liu, X.-Q. He, and W.-T. Xu, "Load restoration optimization considering dynamic constraints during initial period of power system recovery," *Power Syst. Technol.*, vol. 38, no. 9, pp. 2441–2448, Sep. 2014.

[16] K. Deb, A. Pratap, S. Agarwal, and T. Meyarivan, "A fast and elitist multiobjective genetic algorithm: NSGA-II," *IEEE Trans. Evol. Comput.*, vol. 6, no. 2, pp. 182–197, Apr. 2002.

[17] W. Liu, Z. Lin, F. Wen, and G. Ledwich, "A wide area monitoring system based load restoration method," *IEEE Trans. Power Syst.*, vol. 28, no. 2, pp. 2025–2034, May 2013.

[18] H. Gao, Y. Chen, Y. Xu, and C.-C. Liu, "Resilience-oriented critical load restoration using microgrids in distribution systems," *IEEE Trans. Smart Grid*, vol. 7, no. 6, pp. 2837–2848, Nov. 2016.

[19] J. Zhao, H. Wang, Q. Wu, N. D. Hatziargyriou, and F. Shen, "Distributed risk-limiting load restoration for wind power penetrated bulk system," *IEEE Trans. Power Syst.*, vol. 35, no. 5, pp. 3516–3528, Sep. 2020.

[20] L. Sun, Z. Lin, Y. Xu, F. Wen, C. Zhang, and Y. Xue, "Optimal skeleton-network restoration considering generator start-up sequence and load pickup," *IEEE Trans. Smart Grid*, vol. 10, no. 3, pp. 3174–3185, May 2019.

[21] G. H. McDaniel and A. F. Gabrielle, "Load diversity-its role in power system utilization," *IEEE Trans. Power App. Syst.*, vol. PAS-84, no. 7, pp. 626–635, Jul. 1965.

[22] Y. Xu, Y. Wang, J. He, M. Su, and P. Ni, "Resilience-oriented distribution system restoration considering mobile emergency resource dispatch in transportation system," *IEEE Access*, vol. 7, pp. 73899–73912, 2019.

[23] H. Farzin, M. Fotuhi-Firuzabad, and M. Moeini-Aghtaie, "Reliability studies of modern distribution systems integrated with renewable generation and parking lots," *IEEE Trans. Sustain. Energy*, vol. 31, no. 1, pp. 759–768, Jan. 2017.

[24] H. Momen, A. Abessi, and S. Jadid, "Using EVs as distributed energy resources for critical load restoration in resilient power distribution systems," *IET Gener., Transmiss. Distrib.*, vol. 14, no. 18, pp. 3750–3761, Sep. 2020.

[25] M. Wang, P. Zhang, Y. Shi, C. Wu, M. Mammadli, and W. Zhang, "Research on charging load characteristics of EVs based on actual charging power," presented at the Int. Conf. Elect. Eng. Control Technol., Singapore, Dec. 2019.

[26] W.-J. Liu, Z.-Z. Lin, F.-S. Wen, and Y.-S. Xue, "Muti-objective optimal strategies for power system restoration with support with support from electric vehicles," *Automat. Electr. Power Syst.*, vol. 39, no. 20, pp. 32–40, Oct. 2015.

[27] Y. Liu and X.-P. Gu, "Node importance assessment based skeleton-network reconfiguration," *Proc. CSEE*, vol. 27, no. 10, pp. 20–27, Apr. 2007.

[28] Y.-J. Cao, G.-Z. Wang, and L.-H. Zeng, "An identification model for self-organized criticality of power grids based on power flow entropy," *Automat. Electr. Power Syst.*, vol. 35, no. 7, pp. 1–6, Apr. 2011.

[29] L.-H. Yang, Y. Wang, M. Wang, C. Wu, J. Zhou, K.-H. Ji, and R. Chen, "Island division and multi-objective network reconstruction considering power flow entropy," in *Proc. MATEC Web Conf.*, Sanya, China, 2020, pp. 3007–3019.

[30] H. Li and Q. Zhang, "MOEA/D: A multi-objective evolutionary algorithm based on decomposition," *IEEE Trans. Evol. Comput.*, vol. 11, no. 6, pp. 712–731, Nov. 2007.


**MIN WANG** (Member, IEEE) received the Ph.D. degree in power system and its automation from the Hefei University of Technology, Hefei, China, in 2010. She is currently an Associate Professor with the College of Energy and Electrical Engineering, Hohai University, Nanjing, China. Her research interests include renewable energy generation and demand-side response.

**ZONGYIN FAN** (Graduate Student Member, IEEE) received the B.S. degree from the Anhui University of Technology, in 2019. He is currently pursuing the M.S. degree in electrical engineering with Hohai University, Nanjing, China. His research interests include power system network reconstruction and load recovery.

**JIAN ZHOU** was born in Shanghai, China, in 1974. He received the bachelor's degree in applied electronic technology from the Department of Information and Control Engineering, Shanghai Jiaotong University, in 1996, and the master's degree in business administration from Fudan University, in 2013. Since 1996, he has been serving with the Shanghai Electric Power Research Institute of State Grid. He is currently the Deputy Chief Engineer. He has been engaged in power system automation for a long time. His research interests include resilient power grid, power system automation, power system time synchronization, power quality, and so on. He has received many awards for scientific and technological progress of Shanghai and State Grid Corporation.

**SHANSHAN SHI** was born in Anhui, China, in 1985. She received the Ph.D. degree in power systems from Tsinghua University, in 2011. She is currently a Senior Engineer with Tsinghua University. She is also the Director of the Smart Grid Research Office of the Power Grid Technology Center of the State Grid Shanghai Electric Power Research Institute. She has long been engaged in scientific research and development and project management in the fields of distributed power generation, micro-grid, energy storage, and energy Internet. As the project executive or main participant, she has undertaken more than ten national, provincial and ministerial-level scientific and technological projects. Based on research results and practical experience in related fields, in recent years, she has received eight provincial and ministerial awards and ten company awards. She holds a total of 68 patents have been authorized, 36 articles have been published, and six standards have been published.